

Article

Speed Control of Matrix Converter-Fed Five-Phase Permanent Magnet Synchronous Motors under Unbalanced Voltages

Borzou Yousefi ¹, Soodabeh Soleymani ^{1,*}, Babak Mozafari ¹ and Seid Asghar Gholamian ²

¹ Department of Electrical and Computer Engineering, Science and Research Branch, Islamic Azad University (IAU), Tehran 14778-93855, Iran; borzou.yousefi@srbiau.ac.ir (B.Y.); mozafari@srbiau.ac.ir (B.M.)

² Faculty of Electrical and Computer Engineering, Babol Noshirvani University of Technology, Babol 71167-47148, Iran; gholamian@nit.ac.ir

* Correspondence: s.soleymani@srbiau.ac.ir; Tel.: +98-912-333-2659

Academic Editor: Chunhua Liu

Received: 2 August 2017; Accepted: 25 September 2017; Published: 28 September 2017

Abstract: Five-phase permanent magnet synchronous motors (PMSM) have special applications in which highly accurate speed and torque control of the motor are a strong requirement. Direct Torque Control (DTC) is a suitable method for the driver structure of these motors. If in this method, instead of using a common five-phase voltage source inverter, a three-phase to five-phase matrix converter is used, the low-frequency current harmonics and the high torque ripple are limited, and an improved input power factor is obtained. Because the input voltages of such converters are directly supplied by input three-phase supply voltages, an imbalance in the voltages will cause problems such as unbalanced stator currents and electromagnetic torque fluctuations. In this paper, a new method is introduced to remove speed and torque oscillator factors. For this purpose, motor torque equations were developed and the oscillation components created by the unbalanced source voltage, determined. Then, using the active and reactive power reference generator, the controller power reference was adjusted in such a way that the electromagnetic torque of the motor did not change. By this means, a number of features including speed, torque, and flux of the motor were improved in terms of the above-mentioned conditions. Simulations were analyzed using Matlab/Simulink software.

Keywords: permanent magnet synchronous motor; matrix converter; direct power control; unbalanced supply voltage

1. Introduction

Permanent magnet synchronous motors (PMSMs) are similar to ordinary synchronous motors, with the exception that their field winding has been replaced with a permanent magnet. Among these motors, five-phase PMSM has a number of features such as higher efficiency, reliability, and power density than other types of PMSM [1]. These motors are commonly used in special industrial cases such as marine propulsion systems, hybrid vehicles, and the aerospace industry. In most cases, it is necessary to design a proper driver with small size and high reliability [2,3].

One of the common methods to control the torque (and thus finally the speed) of these motor is Direct Torque Control (DTC). The block diagram of the Switching Table based Direct Torque Control (ST-DTC) scheme is shown in Figure 1 [4].

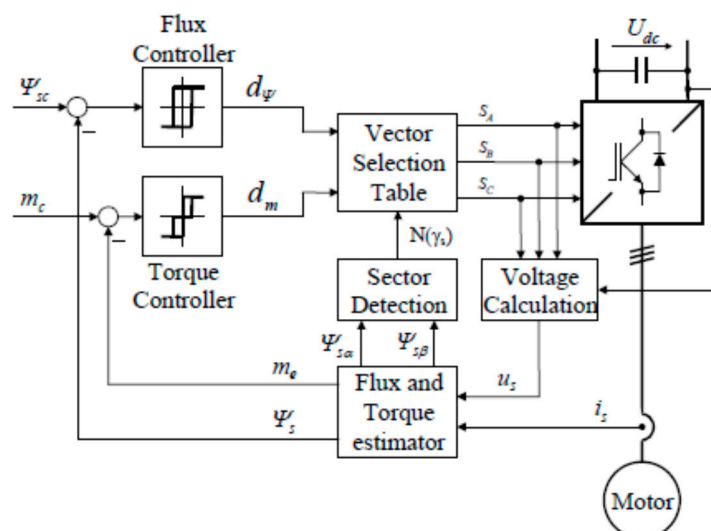


Figure 1. A block diagram of the Switching Table Based Direct Torque Control with circular stator flux path.

The scheme includes two hysteresis controllers. A stator flux controller imposes the time duration of the active voltage vectors, which move the stator flux along the reference trajectory, and the torque controller determines the time duration of the zero voltage vectors, which keep the motor torque in the defined-by-hysteresis tolerance band. Finally, for every sampling time the voltage vector selection block chooses the inverter switching state (S_A , S_B , S_C), which reduces the instantaneous and torque errors.

Figure 2 shows the diagram of a five-phase voltage source inverter which is called the classic method of direct torque control in this article.

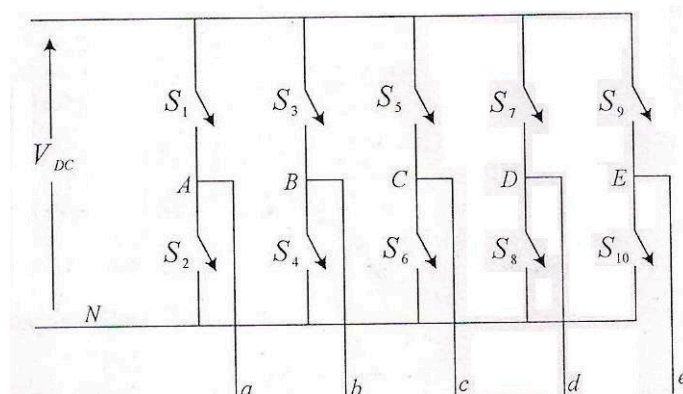


Figure 2. Diagram of a five-phase voltage source inverter.

There are two major drawbacks to applying inverter: low-frequency voltage harmonics and high torque ripple [5–7]. To eliminate these problems, the direct torque control method with a three-phase to five-phase matrix converter (Figure 3) is introduced [8–10]. This circuit is an AC to AC converter. Compared to the VSI converter, intermediate circuits and DC link have been removed [11,12].

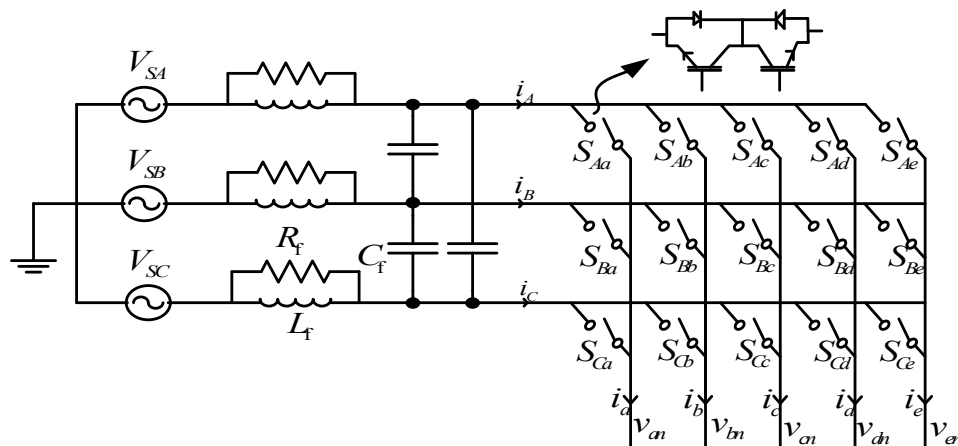


Figure 3. Diagram of a three-phase to five-phase matrix converter.

Using more degrees of freedom in this converter, an optimal switching table is provided, along with the elimination of the mentioned problem, the input power factor is also controlled.

Because the input voltages of the matrix converter are directly supplied by the input voltage source, one of the factors that makes such converters inefficient is the voltage imbalance in the three-phase input supply [13]. In a three-phase system, voltage imbalance usually takes place when the magnitudes or the phase angles of the line voltages are different from the balanced conditions. The voltage imbalance decreases the motor performance. It can also cause current imbalance which is more intense than voltage imbalance. Unbalanced currents lead to torque pulsation and increase losses. Therefore, the power quality and energy efficiency will be reduced [14].

Common causes of voltage imbalance are the faulty operation of the power factor correction equipment, unbalanced or unstable utility supply, unevenly distributed single-phase loads on the same power system, and unidentified single-phase to ground faults.

Because such matrix converters are generally applied where the accurate control of the speed and torque of a motor is considered, developing a new method to eliminate the imbalance impact on process performance is necessary. This paper proposes a direct power control technique to solve this problem. First, the motor power and torque equations are developed and the oscillator phrases which come into existence by voltage imbalance are separated. Then, using an active and reactive power reference generator, the controller power reference is changed so that the machine electromagnetic torque remains constant.

It means that the active and reactive power produced by the generator should properly follow the active and reactive power reference which is favorable. In this way, in addition to optimal speed control, torque oscillator parameters will also be eliminated.

2. Modeling of Five-Phase PMSM and Matrix Converter

The five-phase PMSM stator voltage equation can be expressed as follows:

$$V_s = R_s I_s + \frac{d\Lambda_s}{dt}, \quad \Lambda_s = L_{ss} I_s + \Lambda_m \quad (1)$$

where R_s is the stator resistance matrix, Λ_s is the air gap flux, L_{ss} is the stator inductance matrix including self-inductance and mutual inductance, and Λ_m is the linkage flux matrix which is generated by the permanent magnet and can be expressed as follows:

$$\Lambda_m = \lambda_m [\sin(\theta_r) \sin(\theta_r - 2\pi/5) \sin(\theta_r - 4\pi/5) \sin(\theta_r + 4\pi/5) \sin(\theta_r + 2\pi/5)]^T \quad (2)$$

where λ_m is the value of the permanent magnet flux and θ_r is the rotor position.

For the transfer of the components of a five-phase system from (abcde) space to perpendicular ($\alpha - \beta$) and ($Z_1 - Z_2$) spaces [15], namely ($\alpha - \beta - Z_1 - Z_2$), the following equations are used:

$$f_{\alpha-\beta}^s = \frac{2}{5}(f_{as} + af_{bs} + a^2f_{cs} + a^3f_{ds} + a^4f_{es}) \quad (3)$$

$$f_{z_1-z_2}^s = \frac{2}{5}(f_{as} + a^3f_{bs} + af_{cs} + a^4f_{ds} + a^2f_{es}) \quad (4)$$

In the above equations, $a = \exp(2\pi/5)$. Incorporating Equations (3) and (4) into Equation (1), stator voltages can be expressed as follows:

$$V_{qs} = r_s i_{qs} + \omega \lambda_{qs} + \frac{d\lambda_{qs}}{dt}, V_{ds} = r_s i_{ds} - \omega \lambda_{qs} + \frac{d\lambda_{ds}}{dt}, V_{z_1s} = r_s i_{z_1s} + \frac{d\lambda_{z_1s}}{dt}, V_{z_2s} = r_s i_{z_2s} + \frac{d\lambda_{z_2s}}{dt} \quad (5)$$

where v_{qs} , v_{ds} , v_{z_1s} , and v_{z_2s} are q , d , z_1 , and z_2 axes of voltage of the stator, i_{qs} , i_{ds} , i_{z_1s} , and i_{z_2s} are q , d , z_1 , and z_2 axes of current of the stator, ω is angular velocity, and λ_{qs} , λ_{ds} , λ_{z_1s} , and λ_{z_2s} are q , d , z_1 , and z_2 axes of flux linkage of the stator. They can be expressed as follows:

$$\lambda_{ds} = L_d i_{ds} + \lambda_m, \lambda_{qs} = L_q i_{qs}, \lambda_{z_1s} = L_{ls} i_{z_1s}, \lambda_{z_2s} = L_{ls} i_{z_2s} \quad (6)$$

where L_q and L_d are the inductance of q and d axes, respectively, and L_{ls} is leakage inductance of the stator. The electromagnetic torque can be obtained as follows:

$$T_e = \frac{\partial W_{co}}{\partial \theta_m} \quad (7)$$

where θ_m is the mechanical angle of the rotor and W_{co} is the co-energy. Regardless of other formulas, the final equation for torque is obtained as follows:

$$T_e = \frac{p}{2} \frac{5}{2} [\lambda_m i_{qs} + (L_d - L_q) i_{ds} i_{qs}] \quad (8)$$

In Equation (8), p is the pole pair number. According to the above equation, in a five-phase permanent magnet synchronous motor, only the basic components of the $(\alpha-\beta)$ subspace influence the production of the electromagnetic torque. Thus, in the driver system of this motor, voltage space vectors of this subspace are selected. It should be noted that when a voltage vector of $(\alpha-\beta)$ subspace is chosen, its corresponding vector in the (Z_1-Z_2) subspace will be also stimulated simultaneously.

Having this information, it is possible to easily simulate a five-phase PMSM.

In the next step, the modeling of a five-phase matrix converter will be discussed. The circuit topology of a three-phase to five-phase matrix converter is shown in Figure 3. As can be seen, this converter has five bases; every base has three two-way switches. Each switching function is defined as follows:

$$S_{jk}(t) = \begin{cases} 0 & \text{switch } S_{jk} \text{ is open} \\ 1 & \text{switch } S_{jk} \text{ is closed} \end{cases} \quad j = \{A, B, C\}, k = \{a, b, c, d, e\} \quad (9)$$

where J and k are the input and output phases, respectively.

The converter output voltage vectors in the $(\alpha-\beta)$ and (Z_1-Z_2) subspaces can be obtained by:

$$\begin{cases} V_o^{\alpha-\beta} = \frac{2}{5}(V_a + V_b e^{j\frac{2\pi}{5}} + V_c e^{j\frac{4\pi}{5}} + V_d e^{-j\frac{4\pi}{5}} + V_e e^{-j\frac{2\pi}{5}}) = V_o e^{j\alpha_o} \\ V_o^{Z_1-Z_2} = \frac{2}{5}(V_a + V_b e^{-j\frac{4\pi}{5}} + V_c e^{j\frac{2\pi}{5}} + V_d e^{-j\frac{2\pi}{5}} + V_e e^{j\frac{4\pi}{5}}) = V_o e^{j\alpha_o} \end{cases} \quad (10)$$

where v_o is the size of the output voltage vector and α_o is the phase angle. Generally, there are $3^5 = 243$ switching states in the matrix converter; however, only 93 voltage vectors consisting of

three zero vectors and 90 active vectors which have constant directions can be used. Like the five-phase voltage source inverter (VSI), these 90 vectors form ten concentric regular polygons which are divided into large, medium, and small sizes. Figure 4 shows the voltage vectors in the $(\alpha-\beta)$ and (Z_1-Z_2) subspaces. The numbers shown in this figure correspond to the switching status.

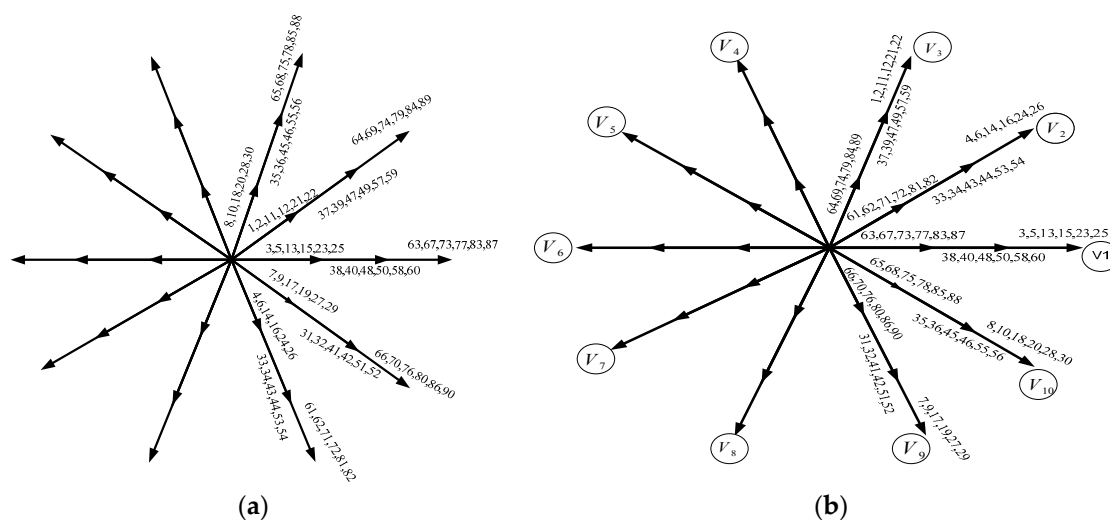


Figure 4. Phase-to-ground voltage output vectors in the subspaces (a) $(\alpha-\beta)$ (b) (Z_1-Z_2) .

3. DTC Method Using a Matrix Converter

The principle of the direct torque control method using a matrix converter is similar to the classic method of direct torque control (using voltage source inverter).

First, the classic direct torque control is done and the inverter output voltage vectors are determined. These vectors are called virtual voltage vectors (vectors v_1 through v_{10} inside the small circle are shown in Figure 4). Then, it must be determined which vectors of the matrix converter can be replaced by the inverter virtual vector. In general, there are six matrix converter voltage vectors for each virtual voltage vector. For example, the vector v_1 means vectors 3, 5, 13, 15, 23, and 25 from the switching status. The next step is to study where the phase-to-ground voltage vectors are located, in which sector of the six vector space. Figure 5 shows the path of the input voltage of a three-phase to a five-phase converter. Knowing the input voltage vector section, and according to Figure 5, the path is divided into six sectors, the first of which starts from $0rad$.

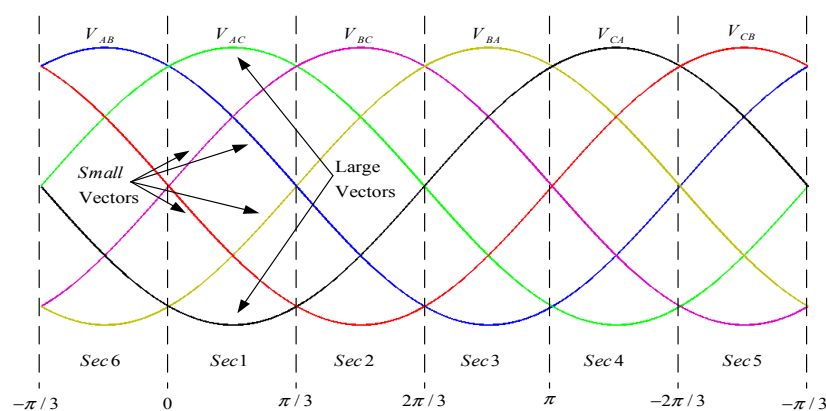


Figure 5. Input voltage vector direction starting from $0rad$.

In this case, there will be six voltage vectors in every sector which do not change their sign in the sector, and thus can be used in the direct torque control method. From among the six vectors, four vectors are small and two vectors are large. Three voltage vectors (two small vectors and one large

vector) can be used in each sector as shown in Figure 5. It can be concluded that compared to classical direct torque control in which only one voltage vector is produced in each sampling cycle, the matrix converter can deliver three voltage vectors. These vectors have the same effect on increasing or decreasing the flux and torque. Therefore, the matrix converter has two more degrees of freedom than the voltage source inverter, which is used to control other parameters of the machine such as power factor and line current THD, therefore, reducing high flux and torque ripples. According to the above statement, a switching table is provided for the direct torque control of the five-phase PMSM, which can be seen as a part of the block diagram of the DTC method using a matrix converter, as shown in Figure 6 [16].

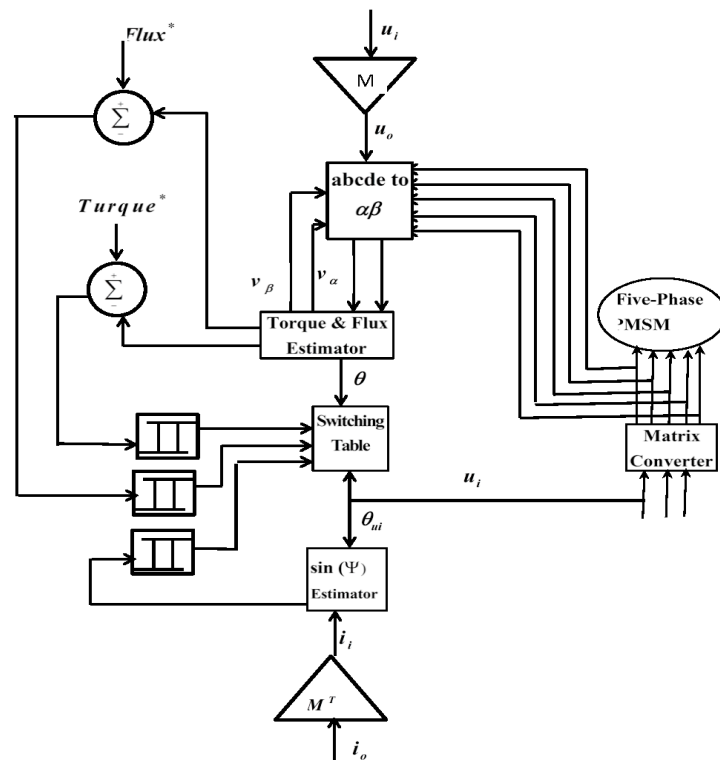


Figure 6. A block diagram of the direct torque control method using a matrix converter.

4. Five-Phase PMSM Control in Terms of Unbalanced Supply Voltage

4.1. Direct Power Control of a Five-Phase PMSM

In the rotor reference frame of PMSM, the voltage of the stator equation can be expressed as follows [17]:

$$V_s^r = R_s I_s^r + \frac{d\phi_s^r}{dt} + j\omega_r \phi_s^r \quad (11)$$

where V_s^r , R_s , and ϕ_s^r represent the stator voltage, resistance, and flux, respectively.

The stator flux linkage vector in the rotor reference frame is expressed as follows:

$$\phi_s^r = L_s I_s^r + \phi_r \quad (12)$$

where L_s is the self-inductance of the stator.

The relationship between the rotor flux and stator flux in the stationary reference system ($\alpha-\beta$) and the rotor reference system ($\alpha_r-\beta_r$) is shown in Figure 7.

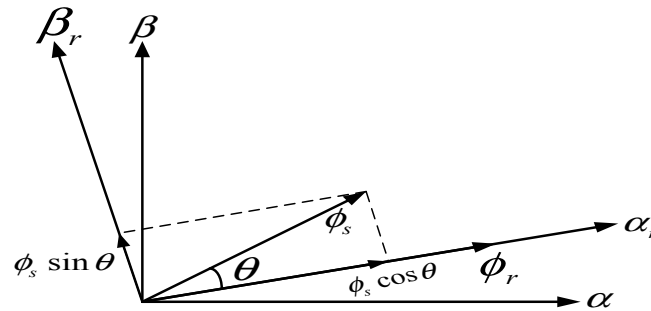


Figure 7. Flux of the rotor and stator flux vector in the rotor and stationary reference frame.

The stator flux in the $(\alpha_r - \beta_r)$ reference frame is expressed as follows:

$$\varphi_s^r = |\varphi_s^r| \cdot e^{j\theta} \quad (13)$$

where θ is the angle of the stator flux in the rotor reference frame, as well as the angle between the stator flux and the rotor flux.

The stator active power Equation is as follows [18]:

$$P_s = \frac{5}{2} V_s^r i_s^r \quad (14)$$

Substituting Equation (11) in Equation (14), and regardless of the stator resistance, P_s can be expressed as follows:

$$P_s = \frac{5}{2} \left(\frac{d\varphi_s^r}{dt} + j\omega_r \varphi_s^r \right) \cdot I_s^r \quad (15)$$

where ω_r is the angular frequency of the rotor.

By deriving Equation (13), Equation (16) can be obtained:

$$\frac{d\varphi_s^r}{dt} = \frac{d|\varphi_s^r|}{dt} \cdot e^{j\theta} + \frac{d\theta}{dt} \cdot j e^{j\theta} \cdot |\varphi_s^r| \quad (16)$$

Referring to Figure 7, the following Equation is obtained:

$$\frac{d\theta}{dt} = \omega_1 - \omega_2 \quad (17)$$

where ω_1 is the stator's angular frequency.

Substituting Equation (17) in Equation (16):

$$\frac{d\varphi_s^r}{dt} = \frac{d|\varphi_s^r|}{dt} \cdot e^{j\theta} + j(\omega_1 - \omega_r) e^{j\theta} \cdot |\varphi_s^r| = \frac{d|\varphi_s^r|}{dt} \cdot e^{j\theta} + j(\omega_1 - \omega_r) \varphi_s^r \quad (18)$$

On the other hand, the stator current in the rotor frame can be calculated using the following Equation:

$$I_s^r = \frac{\varphi_s^r - \varphi_r}{L_s} \quad (19)$$

Using the equations obtained above, the active power Equation can be written as follows:

$$P_s = -\frac{5}{2} \frac{1}{L_s} \omega_r |\varphi_s^r| |\varphi_r| \sin \theta \quad (20)$$

By deriving Equation (19), active power changes are obtained as follows:

$$\frac{dP_s}{dt} = -k_i \omega_r |\varphi_r^r| \frac{d(|\varphi_s^r| \sin \theta)}{dt} \quad (21)$$

Similarly, reactive power is obtained from the following Equation [19]:

$$Q_s = \frac{5}{2} V_s^r \times i_s^r \quad (22)$$

Incorporating equations, Equation (23) is expressed as follows:

$$Q_s = -\frac{5}{2} \left(\frac{d\varphi_s^r}{dt} + j \omega_r \varphi_s^r \right) \times I_s^r \quad (23)$$

As a result, the reactive power Equation can be written as follows:

$$Q_s = \frac{5}{2} \frac{\omega_r}{\sigma L_s} |\varphi_s^r| \left(\frac{L_m}{L_r} |\varphi_r^r| \cos \theta - |\varphi_s^r| \right) \quad (24)$$

and similar to Equation (21), the reactive power changes are obtained as follows:

$$\frac{dQ_s}{dt} = k_i \omega_r |\varphi_r^r| \frac{d(|\varphi_s^r| \cos \theta)}{dt} \quad (25)$$

According to Equations (21) and (25), rapid changes of active and reactive power can be made by changes in $|\varphi_s^r| \sin \theta$ and $|\varphi_s^r| \cos \theta$ respectively. It can be seen from Figure 7 that $|\varphi_s^r| \sin \theta$ and $|\varphi_s^r| \cos \theta$ are the components of the stator flux φ_s^r , perpendicular to the rotor flux, and in the direction of the rotor flux, respectively. This shows that, if the stator flux variation is in the direction of the rotor flux, namely $|\varphi_s^r| \cos \theta$, reactive power Q_s changes. Similarly, if the stator flux variation is perpendicular to the rotor flux, namely $|\varphi_s^r| \sin \theta$, active power P_s changes.

4.2. Investigating the Effect of Two-Level Inverter Voltage Vectors on Active and Reactive Power Changes

To study the effect of voltage vectors, the vector space of voltages of a two-level inverter is divided into six sectors, each sector covers 60 degrees [20]. This is illustrated in Figure 8.

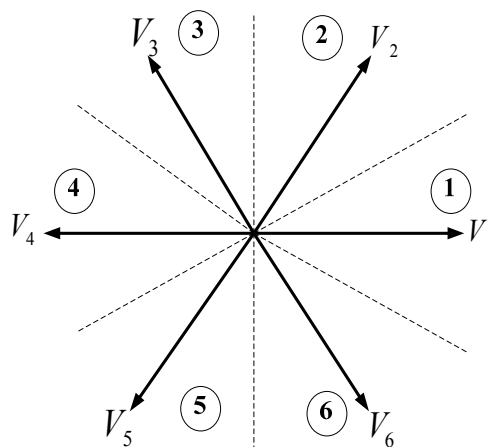


Figure 8. Six vector sectors of a three-phase voltage source inverter.

In reference [21], the effect of voltage vectors on active and reactive power changes was investigated.

According to Figure 9, suppose that the stator flux vector in the reference frame of the rotor (φ_{s1}^r) is located in the second section of the vector space. As shown in this figure, this vector leads the rotor flux vector by θ_1 degrees. Now, if the voltage vector V_1 is applied to the converter, the position of

the stator flux vector is changed and moved to ϕ_{s2}^r . It can be seen that by applying the voltage vector V_1 to the converter, the value of $\phi_s^r \sin \theta$ decreases and the value of $\phi_s^r \cos \theta$ increases. As a result, with respect to the Equations (21) and (25), the active and reactive power increases.

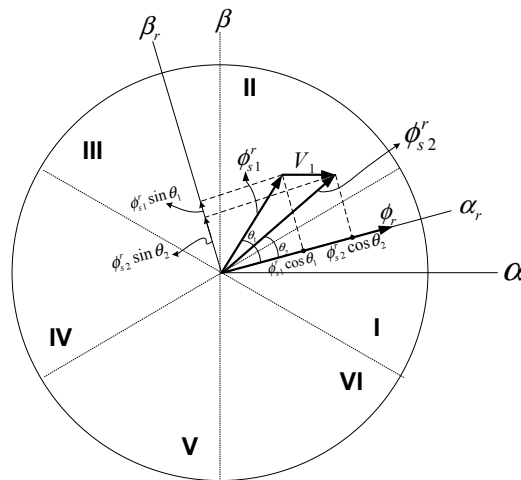


Figure 9. Effect of vector V_1 on active and reactive power changes.

In the same way, knowing the position of the stator flux in the rotor reference frame, the effect of all voltage vectors on active and reactive power changes can be studied. According to the example, a switching table can be prepared and used for different modes.

4.3. Vector Space under Imbalance Conditions

In this section, an imbalance caused by an unbalanced load is studied. An asymmetric five-phase system can be decomposed into five symmetrical systems of five phases. These five systems are called the sequence of zero, positive sequence ($\alpha-\beta$) subspace, negative sequence ($\alpha-\beta$) subspace, positive sequence (Z_1-Z_2) subspace, and negative sequence (Z_1-Z_2) subspace. They can be obtained by,

$$\begin{bmatrix} x^0 & x_{\alpha-\beta}^+ & x_{\alpha-\beta}^- & x_{\alpha-\beta}^+ & x_{\alpha-\beta}^- \end{bmatrix}^T = \frac{1}{5} \begin{bmatrix} 1 & 1 & 1 & 1 & 1 \\ 1 & a & a^2 & a^3 & a^4 \\ 1 & a^4 & a^3 & a^2 & a \\ 1 & a^3 & a & a^4 & a^2 \\ 1 & a^2 & a^4 & a & a^3 \end{bmatrix} \begin{bmatrix} x_a \\ x_b \\ x_c \\ x_d \\ x_e \end{bmatrix} \quad (26)$$

where $a = e^{j(2\pi/5)}$. Parameters x_a, x_b, x_c, x_d , and x_e represent the unbalanced system. Parameters $x^0, x^+,$ and x^- represent zero, positive, and negative sequence components, respectively. It is assumed that the five-phase system being studied is a five-wire five-phase system. This means that the system does not have a neutral wire. In this case, the sum of the five-phase currents is always equal to zero ($i_a + i_b + i_c + i_d + i_e = 0$). As a result, the zero sequence current component would be equal to zero. Consequently, the components of the zero sequence voltage are zero ($v_a + v_b + v_c + v_d + v_e = 0$).

Therefore, to take into account the positive and negative sequence, the voltage and current vectors can be expressed as follows:

$$\begin{cases} \vec{v} = (\vec{v}^+ + \vec{v}^-) = v_\alpha + jv_\beta = (v_\alpha^+ + jv_\beta^+) + j(v_\beta^+ + v_\alpha^+), \vec{v} = (\vec{v}^+ + \vec{v}^-) = v_{\alpha 1} + jv_{\alpha 2} = (v_{\alpha 1}^+ + jv_{\alpha 2}^+) + j(v_{\alpha 2}^+ + v_{\alpha 1}^+) \\ \vec{i} = (\vec{i}^+ + \vec{i}^-) = i_\alpha + ji_\beta = (i_\alpha^+ + ji_\beta^+) + j(i_\beta^+ + i_\alpha^+), \vec{i} = (\vec{i}^+ + \vec{i}^-) = i_{\alpha 1} + ji_{\alpha 2} = (i_{\alpha 1}^+ + ji_{\alpha 2}^+) + j(i_{\alpha 2}^+ + i_{\alpha 1}^+) \end{cases} \quad (27)$$

Thus, two space vector of the five-phase system can be expressed as follows:

$$\overrightarrow{x_{\alpha-\beta}} = x_{\alpha} + jx_{\beta} = \frac{2}{5}(x_a + ax_b + a^2x_c + a^3x_d + a^4x_e), \overrightarrow{x_{z1-z2}} = x_{z1} + jx_{z2} = \frac{2}{5}(x_a + a^3x_b + ax_c + a^4x_d + a^2x_e) \quad (28)$$

A five-phase unbalanced system can be demonstrated as the sum of positive and negative sequences as follows:

An unbalanced five-phase system can be represented as the sum of two positive and negative sequence vectors that rotate in the opposite direction with the same frequency as follows:

$$\vec{x} = \vec{x}^+ + \vec{x}^- = |\vec{x}^+|e^{j(\omega t + \theta^+)} + |\vec{x}^-|e^{-j(\omega t + \theta^-)} \quad (29)$$

4.4. Direct Power Control

Figure 10 shows a block diagram of the direct power control method of a five-phase PMSM.

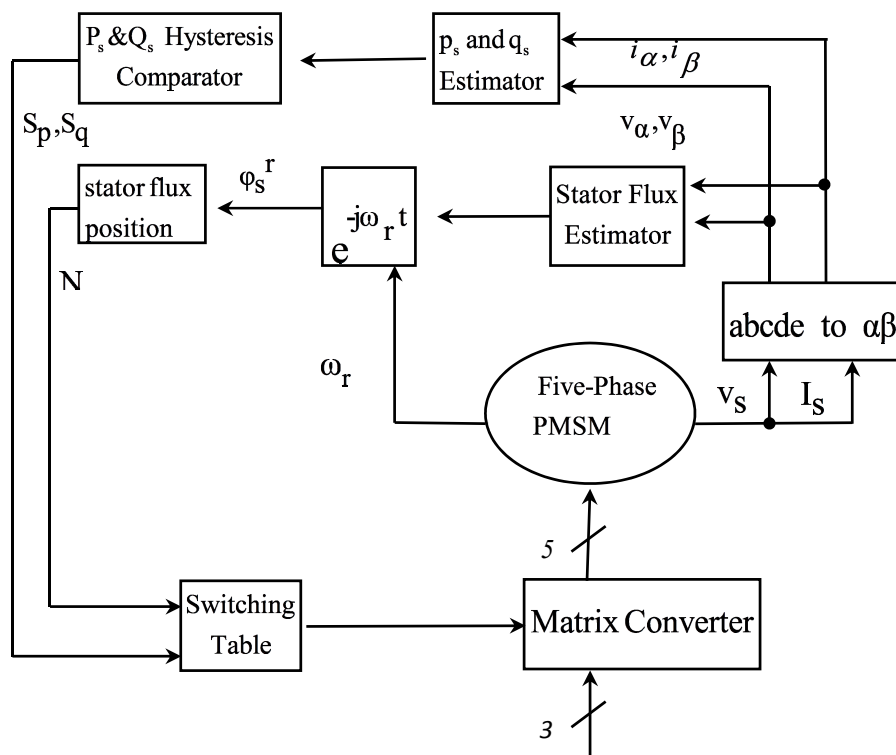


Figure 10. A block diagram of direct power control.

It can be seen from the figure that the voltage and current are sampled from the stator and transmitted to the stationary reference frame. Then, using these voltages and currents, active and reactive powers can be calculated. Moreover, the size of the stator flux and its angle are obtained using the following Equation [22]:

$$\varphi_s = \int (V_s - R_s I_s) dt, \varphi_s = \tan^{-1} \left(\frac{\varphi_\beta}{\varphi_\alpha} \right) \quad (30)$$

The stator flux obtained from the synchronous reference frame is transmitted to the rotor reference frame and φ_s^r is calculated. Then, according to the angle of the flux, the region where the flux vector is located is obtained (with N as shown in Figure 10). In general, the purpose of the direct power control method is that the active and reactive power of the motor properly follow the favorable active and reactive power references. In order to achieve this, the estimated power values are compared with the reference values, and their differences are transmitted to two three-level hysteresis comparators, which are described below.

4.5. Three-Level Hysteresis Comparators

To determine the status of active and reactive power, the three-level hysteresis comparators are used as shown in Figure 11.

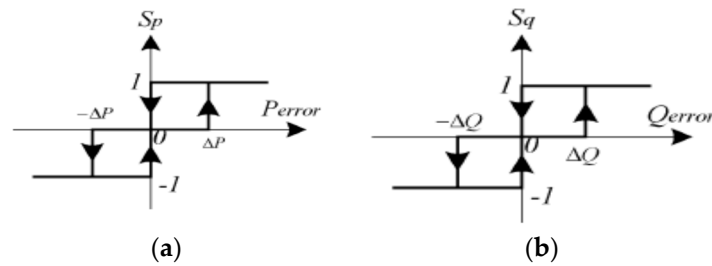


Figure 11. Three-level hysteresis comparators: (a) active power; (b) reactive power.

The difference between the actual value of the power and the reference value is expressed by:

$$P_{error} = P^* - P, \quad Q_{error} = Q^* - Q, \quad (31)$$

In this equation, the reference values of the active and reactive power are shown by P^* and Q^* , respectively.

These error values are sent to the comparators and, according to the allowable band of error, they produce suitable active and reactive power shown as S_p and S_q , respectively.

If this difference is greater than the permitted error value that is interpreted as the allowed band, the comparator output sends the digital number (1), and if the error is in its allowed band, the comparator output sends the digital number (0).

Also, if the error is less than the allowed band, the comparator output sends the digital number (-1).

4.6. Analysis of Five-Phase PMSM under Imbalance Conditions

The five-phase PMSM stator voltage equation was given in Equation (1). From Equations (1) and (8), the torque equation can also be expressed as follows:

$$T_e = \frac{5}{2} \rho \operatorname{Im} \{ \vec{\lambda}_s^* \cdot \vec{i}_s^- \} = \frac{p}{2} \frac{5}{2} [\lambda_{\alpha} i_{\beta} - \lambda_{\beta} i_{\alpha}] \quad (32)$$

where ρ is the derivative operator and “*” sign represents the conjugate of each complex vector. When the stator voltage is unbalanced, all vectors in Equation (1) have a positive and negative sequence. Firstly, the effect of unbalanced voltages on the stator flux is studied. From Equations (1) and (27), the relationship between the stator flux and voltage can be expressed as follows:

$$V_s^+ = r_s i_s^+ + j\omega \lambda_s^+, \quad V_s^- = r_s i_s^- - j\omega \lambda_s^- \quad (33)$$

As can be seen from Figure 12, the stator flux includes two sets of positive and negative components that rotate in opposite directions.

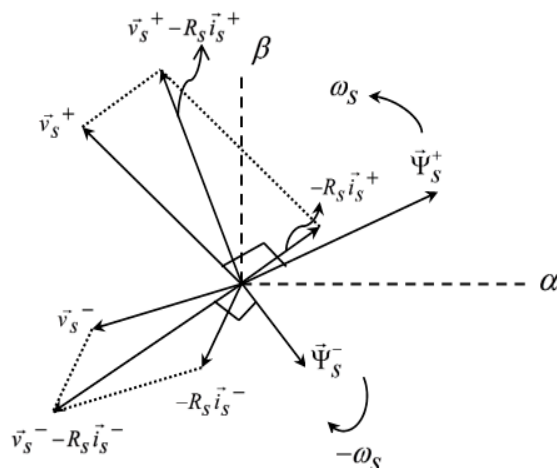


Figure 12. Relationship between fluxes, voltage, and current vectors of stator.

Substituting the components of the positive and negative sequence of the stator flux and current in Equation (32), the following equation is obtained:

$$T_e = \frac{5}{2} \rho \operatorname{Im} \left\{ \overline{\lambda_s^+} \cdot i_s^+ + \overline{\lambda_s^+} \cdot i_s^- + \overline{\lambda_s^-} \cdot i_s^+ + \overline{\lambda_s^-} \cdot i_s^- \right\} \quad (34)$$

It can be seen that the electromagnetic torque consists of two constant phrases (phrases that are the product of identical sequences) and two phrases at 2ω speed (phrases that are the product of different sequences).

Thus, substituting Equation (33) in Equation (34), the following Equation is obtained:

$$T_e = \frac{5}{2} \rho \frac{1}{\omega} \operatorname{Re} \left\{ \overline{v_s^+} \cdot i_s^{+*} - \overline{v_s^-} \cdot i_s^{+*} - \overline{v_s^+} \cdot i_s^{-*} + \overline{v_s^-} \cdot i_s^{-*} - R_s \left(|i_s^+|^2 - |i_s^-|^2 \right) \right\} \quad (35)$$

Equation (35) can be expressed as follows:

$$T_e = \frac{P}{\omega} (A_{s-T} - B_{s-T} + C_{s-T} - D_{s-T} - E_{s-T}) \quad (36)$$

which A_{s-T} , B_{s-T} , C_{s-T} , D_{s-T} , and E_{s-T} are:

$$\begin{cases} A_{s-T} = \frac{5}{2} \operatorname{Re} \left\{ \overline{V_s^+} \cdot i_s^{+*} \right\} = \frac{5}{2} (v_\alpha^+ i_\alpha^+ + v_\beta^+ i_\beta^+), B_{s-T} = \frac{5}{2} \operatorname{Re} \left\{ \overline{V_s^-} \cdot i_s^{+*} \right\} = \frac{5}{2} (v_\alpha^- i_\alpha^+ + v_\beta^- i_\beta^+) \\ C_{s-T} = \frac{5}{2} \operatorname{Re} \left\{ \overline{V_s^+} \cdot i_s^{-*} \right\} = \frac{5}{2} (v_\alpha^+ i_\alpha^- + v_\beta^+ i_\beta^-), D_{s-T} = \frac{5}{2} \operatorname{Re} \left\{ \overline{V_s^-} \cdot i_s^{-*} \right\} = \frac{5}{2} (v_\alpha^- i_\alpha^- + v_\beta^- i_\beta^-), E_{s-T} = R_s \left(|i_s^+|^2 - |i_s^-|^2 \right) \end{cases} \quad (37)$$

The relationship between active and reactive power can be expanded as follows:

$$\overline{S}(t) = P(t) + jQ(t) = \frac{5}{2} (\overline{v_s^+} \cdot i_s^{+*} + \overline{v_s^-} \cdot i_s^{+*} + \overline{v_s^+} \cdot i_s^{-*} + \overline{v_s^-} \cdot i_s^{-*}) \quad (38)$$

The active power equation extracted from Equation (38) can be expressed as follows:

$$P = (A_{s-p} + B_{s-p} + C_{s-p} + D_{s-p}) \quad (39)$$

which A_{s-p} , B_{s-p} , C_{s-p} , and D_{s-p} are:

$$\begin{cases} A_{s-p} = \frac{5}{2} \operatorname{Re} \left\{ \overline{V_s^+} \cdot i_s^{+*} \right\} = \frac{5}{2} (v_\alpha^+ i_\alpha^+ + v_\beta^+ i_\beta^+), B_{s-p} = \frac{5}{2} \operatorname{Re} \left\{ \overline{V_s^-} \cdot i_s^{+*} \right\} = \frac{5}{2} (v_\alpha^- i_\alpha^+ + v_\beta^- i_\beta^+) \\ C_{s-p} = \frac{5}{2} \operatorname{Re} \left\{ \overline{V_s^+} \cdot i_s^{-*} \right\} = \frac{5}{2} (v_\alpha^+ i_\alpha^- + v_\beta^+ i_\beta^-), D_{s-p} = \frac{5}{2} \operatorname{Re} \left\{ \overline{V_s^-} \cdot i_s^{-*} \right\} = \frac{5}{2} (v_\alpha^- i_\alpha^- + v_\beta^- i_\beta^-) \end{cases} \quad (40)$$

Similarly, the reactive power Equation can be expressed as follows:

$$Q=(A_{s-Q}+B_{s-Q}+C_{s-Q}+D_{s-Q}) \quad (41)$$

which A_{s-Q} , B_{s-Q} , C_{s-Q} , and D_{s-Q} are:

$$\begin{cases} A_{s-Q} = \frac{5}{2} \text{Im} \left\{ \overline{V_s^+} \cdot i_s^{+*} \right\} = \frac{5}{2} (v_\beta^+ i_\alpha^+ - v_\alpha^+ i_\beta^+), B_{s-Q} = \frac{5}{2} \text{Im} \left\{ \overline{V_s^-} \cdot i_s^{-*} \right\} = \frac{5}{2} (v_\beta^- i_\alpha^- - v_\alpha^- i_\beta^-) \\ C_{s-Q} = \frac{5}{2} \text{Im} \left\{ \overline{V_s^+} \cdot i_s^{-*} \right\} = \frac{5}{2} (v_\beta^+ i_\alpha^- - v_\alpha^+ i_\beta^-), D_{s-Q} = \frac{5}{2} \text{Im} \left\{ \overline{V_s^-} \cdot i_s^{+*} \right\} = \frac{5}{2} (v_\beta^- i_\alpha^+ - v_\alpha^- i_\beta^+) \end{cases} \quad (42)$$

As can be seen from Equation (37), C_{s-T} and D_{s-T} are oscillating factors in the electromagnetic torque, since they include voltage and current components with two different sequences.

Similarly, according to Equations (40) and (41), C_{s-P} , D_{s-P} , C_{s-Q} and D_{s-Q} cause fluctuations in the active and reactive power, respectively.

Meanwhile, according to Equations (37) and (40), it can be seen that $C_{s-T} = C_{s-P}$ and $D_{s-T} = D_{s-P}$.

As a result, the oscillating factors of the active power and the electromagnetic torque are similar.

In the following, it is first studied whether the electromagnetic torque fluctuations will be eliminated by eliminating the active and reactive power oscillators. Otherwise, because the priority is to eliminate the electromagnetic torque fluctuations, the conditions to eliminate the oscillator of the electromagnetic torque are applied and under these conditions, new references for active and reactive powers will be obtained.

4.7. Remove Power Oscillator Factor

According to Figure 13, and as previously mentioned, a reference value is considered to control the power. The controller must act so that the stator powers properly follow the reference power. Because there is an imbalance in the source voltage, the controller must adjust the source reference so that it creates a new reference power. In Figure 13, the primary reference power (before an imbalance) is shown as ($P_{-required}$) and the new reference power (after an imbalance) is shown as (P_{ref}).

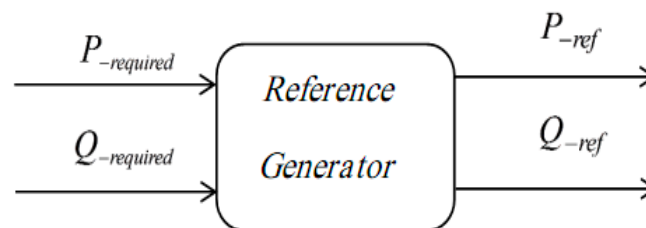


Figure 13. Production of the new power sources in an imbalance condition.

It can be seen from Equation (39) that for the production of constant active power, the sum of two oscillator factors (C_{s-P} , D_{s-P}) must be zero as follows:

$$C_{s-P} + D_{s-P} = 0 \quad (43)$$

Also based on Equation (41), for the production of constant reactive power, the sum of two oscillator factors (C_{s-Q} , D_{s-Q}) must be zero as follows:

$$C_{s-Q} + D_{s-Q} = 0 \quad (44)$$

Since each of the values C_{s-P} , D_{s-P} , C_{s-Q} , and D_{s-Q} is dependent on the positive and negative sequence components, none of them can be zero by itself. In that case, the stator current should be zero, which is not desirable. Therefore, only their sum can be zero. ($C_{s-P} + D_{s-P} = 0$ and $C_{s-Q} + D_{s-Q} = 0$).

In this condition the reference powers before and after an imbalance will also be equal as follows:

$$P_{required} = P_{ref} = A_{s-p} + B_{s-p} \quad (45)$$

$$Q_{required} = Q_{ref} = A_{s-Q} + B_{s-Q} \quad (46)$$

The torque equation can also be obtained as follows:

$$T_e = \frac{P}{\omega} (A_{s-T} - B_{s-T} + 2C_{s-p} - E_{s-T}) = \frac{P}{\omega} (A_{s-T} - B_{s-T} - 2D_{s-p} - E_{s-T}) \quad (47)$$

As can be seen from Equation (45), torque oscillator factors are still present, which is not desirable.

It should be noted that the main goal is to obtain a constant torque in imbalance conditions, not constant power.

4.8. Remove Torque Oscillator Factor

According to Equation (36), the only way to eliminate the torque oscillator factors is obtained under the following conditions:

$$C_{s-T} - D_{s-T} = 0 \quad (48)$$

As a result, the electromagnetic torque value can be obtained as follows:

$$T_e = \frac{P}{\omega} (A_{s-T} - B_{s-T} - E_{s-T}) \quad (49)$$

In this condition, the relationship between reference powers before and after an imbalance condition is as follows:

$$P_{ref} = P_{required} + 2C_{s-p} = P_{required} + 2D_{s-p} \quad (50)$$

$$Q_{required} = Q_{ref} = A_{s-Q} + B_{s-Q} \quad (51)$$

Based on Equations (50) and (51), the controller should operate so that the motor powers properly follow the new reference powers and the motor is used in constant torque and consequently in constant speed.

5. Simulation Results

In this section, the speed control of a matrix converter-fed five-phase PMSM under an unbalanced input voltage, which is improved with the proposed method in this paper, is simulated using Matlab/Simulink software. The steady-state and dynamic performance of the motor is studied. The results are compared with those of a three-phase supply input voltage unbalanced network without correction. The motor's parameter is shown in Table 1.

Table 1. Characteristics of five-phase permanent magnet motor.

Parameter	Symbol	Value
Pole	P	2
Reference speed	N	600 R.P.M
D-axis inductance	L_d	18 mh
q-axis inductance	L_q	42 mh
Stator resistance	r_s	0.7 Ω
Inertia	J	0.01
Coefficient of friction	B	0.005
Motor permanent magnet flux	ϕ_f	0.5 wb
Load torque	T_L	10 N.m

An unbalanced three-phase voltage source can be created in different states, such as differences in amplitude, phase, frequency, and/or all of them.

Figure 14 illustrates an unbalanced three-phase source whose amplitude of phase “A” is different from other phases.

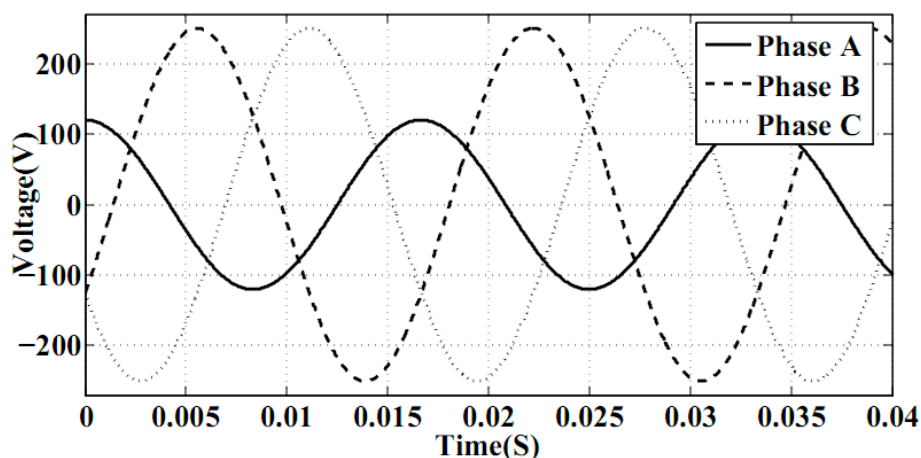


Figure 14. Unbalanced three-phase voltage source.

Other characteristics of the source (phase and frequency) are the same as a normal three-phase power supply. This happens when the phase area is loaded by separate single phased appliances connected to a typical three-phase input. Also a short part of the time (0.04 s) is selected.

Figure 15 illustrates the simulation results with the proposed method under the above-mentioned conditions.

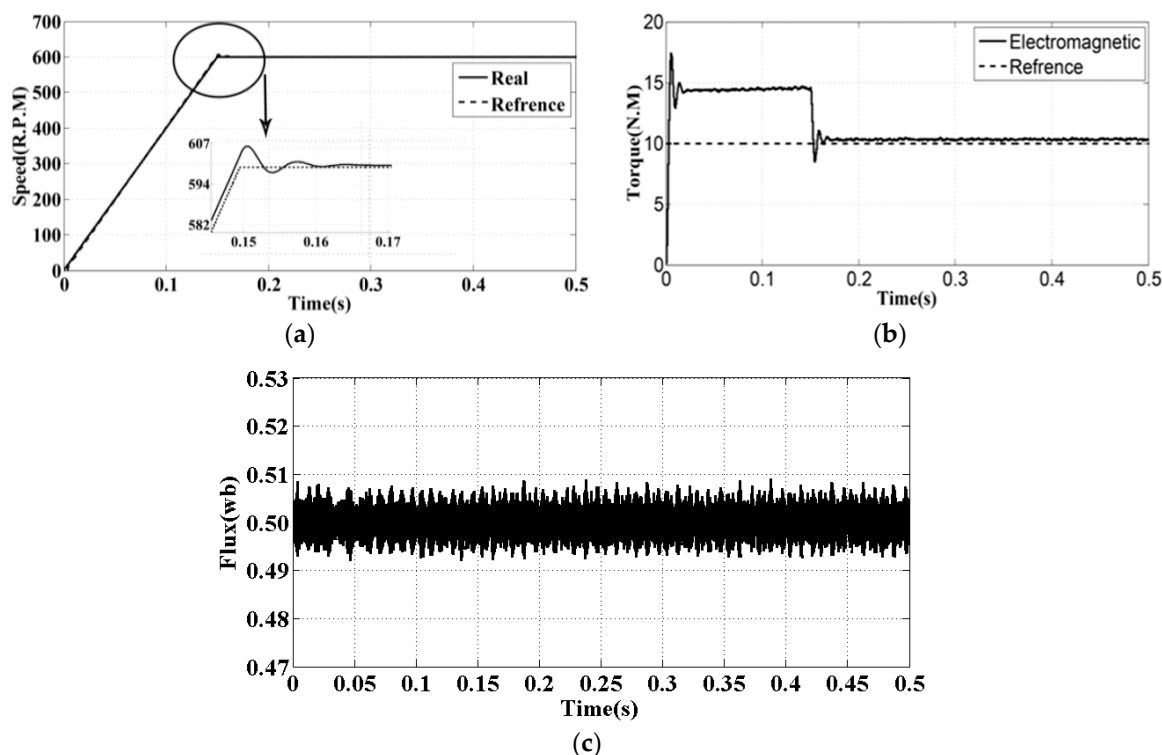


Figure 15. Characteristics of the motor compared with the reference. (a) Speed of the motor; (b) Electromagnetic torque; (c) stator flux in the α axis of the stationary frame.

As shown in Figure 15a, the motor speed will follow its reference value properly. The reference speed value is 600 R.P.M. and the results are shown in Table 2.

Table 2. Characteristics of the motor speed curve.

Parameter	Value
Rise Time	0.1181
Settling Time	0.1461
Settling Min	540
Settling Max	606.4635
Overshoot	1.0850
Undershoot	1.7385
Peak	606.4635
Peak Time	0.1513

Figure 15b shows the load torque in comparison with the electromagnetic torque. The load torque value is 10 N.M. The information obtained from simulation is shown in Table 3.

Table 3. Characteristics of the motor torque curve.

Parameter	Value
Rise Time	0.0018
Settling Time	0.6517
Settling Min	8.4863
Settling Max	17.4246
Overshoot	69.5143
Undershoot	0.2335
Peak	17.4246
Peak Time	0.0057

Figure 15c demonstrates the stator flux diagram on the α axes of stationary frame. It should be noted that the reference flux is equal to the motor permanent magnet flux and is considered to be 0.5 (wb). This figure shows that the stator flux will follow its reference value properly. The information was obtained from simulation is shown in Table 4.

Table 4. Characteristics of the motor flux curve.

Parameter	Value
Rise Time	1.9811×10^{-5}
Settling Time	3
Settling Min	0.4917
Settling Max	0.5091
Overshoot	1.3884
Undershoot	0
Peak	0.5091
Peak Time	2.1875

Figure 16 shows the same characters of the motor as in Figure 15 under the same input conditions, but without using the imbalance correction method.

Figure 16a illustrates the motor speed without using the correction method. The information obtained from simulation is shown in Table 5.

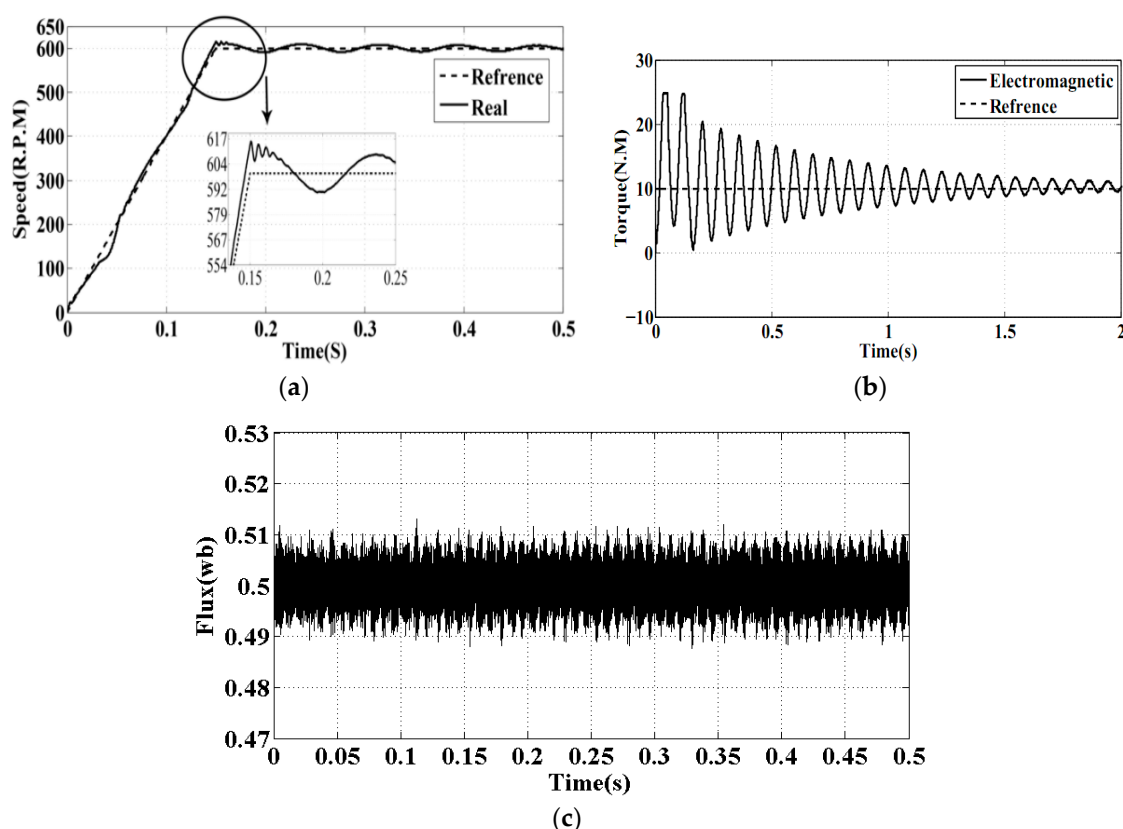


Figure 16. Characteristics of the motor compared with the reference (without correction). (a) Speed of the motor; (b) electromagnetic torque; (c) stator flux in the α axis of the stationary frame.

Table 5. Characteristics of the motor speed curve without using the correction method.

Parameter	Value
Rise Time	0.1175
Settling Time	0.1619
Settling Min	539.9668
Settling Max	615.8829
Overshoot	2.6581
Undershoot	0.0143
Peak	615.8829
Peak Time	0.1508

As shown in Table 5, a lot of the motor speed characteristics as settling time, settling max, overshoot and peak value are more than Figure 15a.

Figure 16b shows the load torque in comparison with the electromagnetic torque without using the correction method. The information obtained from simulation is shown in Table 6.

Table 6. Characteristics of the motor torque curve without using the correction method.

Parameter	Value
Rise Time	0.0162
Settling Time	2.9891
Settling Min	0.4657
Settling Max	24.9209
Overshoot	143.8072
Undershoot	0.3182
Peak	24.9209
Peak Time	0.0462

As shown in Table 5, also a lot of motor torque characteristics as settling time, settling max, overshoot and peak value are more than Figure 15b.

Figure 16c demonstrates the stator flux diagram on the α axes of the stationary frame without using the correction method. The information obtained from simulation is shown in Table 7.

Table 7. Characteristics of the motor flux curve without using the correction method.

Parameter	Value
Rise Time	1.8018×10^{-5}
Settling Time	3
Settling Min	0.4877
Settling Max	0.5130
Overshoot	1.9681
Undershoot	0
Peak	0.5130
Peak Time	0.1124

According to Table 7, the overshoot of motor flux is increased and there is a worse situation than previously.

To evaluate the motor performance with the proposed method in dynamic conditions, a step load at the reference speed of 600 (RPM) is applied to the motor (Figure 17).

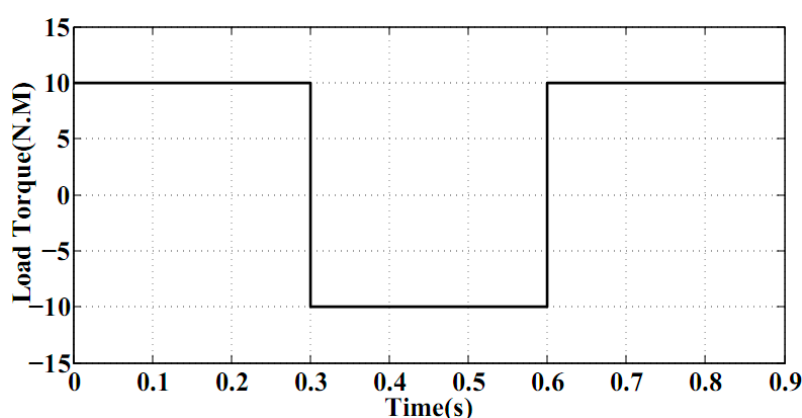
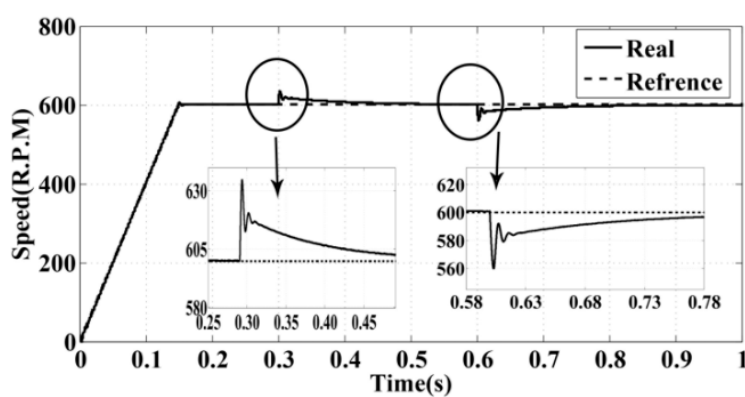


Figure 17. The step load applied to the motor.

According to this figure, the torque load direction was changed between 0.3 to 0.6 s. Figure 18 illustrates the motor characteristics.



(a)

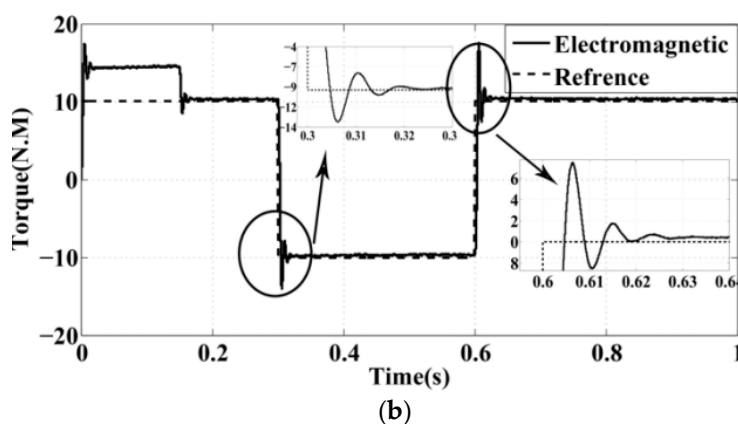


Figure 18. Characteristics of the motor compared with the reference (with applying step load). (a) Speed of the motor; (b) electromagnetic torque.

As shown in Figure 18a, the motor speed follows its reference value properly. The reference speed value is 600 R.P.M. the information obtained from simulation is shown in Table 8.

Table 8. Characteristics of the motor speed curve.

Parameter	Value
Rise Time	0.1181
Settling Time	0.6424
Settling Min	540
Settling Max	634.7243
Overshoot	5.7967
Undershoot	1.7385
Peak	634.7243
Peak Time	0.3028

Figure 18b shows the load torque in comparison with the electromagnetic torque. The load torque value is 10 N.M. the information obtained from simulation is shown in Table 9.

Table 9. Characteristics of the motor torque curve.

Parameter	Value
Rise Time	0.0018
Settling Time	0.6170
Settling Min	−13.9769
Settling Max	17.4974
Overshoot	70.0334
Undershoot	135.8224
Peak	17.4974
Peak Time	0.6063

6. Conclusions

In this paper, a new technique is proposed to eliminate the unbalanced three-phase voltage source effect on a five-phase permanent magnet motor performance that uses a matrix converter in its driver structure. This method is based on direct power control. Because of the imbalance in the voltage source, the motor torque and speed will fluctuate. By identifying the torque oscillation factors and by eliminating these factors, the motor power reference changes. A reference generator has the task of generating a new power reference every time. With a control unit, the active and reactive

powers of the motor properly follow the new active and reactive power references. Each time the reference power changes, however, the torque and speed characteristics remain constant.

Author Contributions: Borzou Yousefi surveyed the backgrounds of the research and proposed the main idea. Soodabeh Soleymani, Babak Mozafari and Seid Asghar Gholamian contributed to the simulation and the modeling and controller design. The authors worked collectively on the manuscript preparation.

Conflicts of Interest: The authors declare no conflict of interest.

References

1. Zhao, J.; Liu, W.; Li, B.; Liu, X.; Gao, C.; Gu, Z. Investigation of Electromagnetic, Thermal and Mechanical Characteristics of a Five-Phase Dual-Rotor Permanent-Magnet Synchronous Motor. *Energies* **2015**, *8*, 9688–9718.
2. Yu, F.; Cheng, M.; Chau, K.T.; Li, F. Control and Performance Evaluation of Multiphase FSPM Motor in Low-Speed region for Hybrid Electric Vehicles. *Energies* **2015**, *8*, 10335–10353.
3. Wu, X.; Wang, H.; Huang, S.; Huang, K.; Wang, L. Sensorless Speed Control with Initial Rotor Position Estimation for Surface Mounted Permanent Magnet Synchronous Motor Drive in Electric Vehicles. *Energies* **2015**, *8*, 11030–11046.
4. Kazmierkowski, M.P.; Buja, G. Review of direct torque control methods for voltage source inverter-fed induction motors. In Proceedings of the 29th Annual Conference of the IEEE—Industrial Electronics Society, 2003. IECON '03, Roanoke, VA, USA, 2–6 November 2003.
5. Loncarski, J.; Leijon, M.; Srndovic, M.; Rossi, C.; Grandi, G. Comparison of Output Current Ripple in Single and Dual Three-Phase Inverters for Electric Vehicle Motor Drives. *Energies* **2015**, *8*, 3832–3848.
6. Cai, X.J.; Wu, Z.X.; Li, Q.F.; Wang, S.X. Phase-Shifted Carrier Pulse Width Modulation Based on Particle Swarm Optimization for Cascaded H-bridge Multilevel Inverters with Unequal DC Voltages. *Energies* **2015**, *8*, 9670–9687.
7. Liu, X.; Du, J.; Liang, D. Analysis and Speed Ripple Mitigation of a Space Vector Pulse Width Modulation-Based Permanent Magnet Synchronous Motor with a Particle Swarm Optimization Algorithm. *Energies* **2016**, *9*, 923.
8. Bak, Y.; Lee, E.; Lee, K.B. Indirect Matrix Converter for Hybrid Electric Vehicle Application with Three-Phase and Single-Phase Outputs. *Energies* **2015**, *8*, 3849–3866.
9. Yongchang, J. Direct torque control of permanent magnet synchronous motor with reduced torque ripple and commutation frequency. *IEEE Trans. Power Electron.* **2011**, *26*, 235–248.
10. Ortega, C.; Arias, A.; Caruana, C.; Balcels, J. Improved waveform quality in direct torque control of matrix-converter-fed PMSM drives. *IEEE Trans. Ind. Electron.* **2010**, *57*, 2101–2110.
11. Tuyen, N.D.; Dzung, P.Q. Space Vector Modulation for an Indirect Matrix Converter with Improved Input Power Factor. *Energies* **2017**, *10*, 588.
12. Yousefi Talouki, A.; Gholamian, S.A.; Yousefi Talouki, M. Harmonic elimination in switching-table based direct torque control of Five-Phase PMSM using matrix coneveptr. In Proceedings of the 2012 IEEE Symposium on Humanitys, Science and Engineering Research, Kuala Lumpur, Malaysia, 24–27 June 2012; pp. 777–782.
13. Mendes, V.F.; Matos, F.F.; Liu, S.Y.; Cupertino, A.F.; Pereira, H.A.; De Sousa, C.V. Low Voltage Ride-Through Capability Solutions for Permanent Magnet Synchronous Wind Generators. *Energies* **2016**, *9*, 59.
14. Zhao, J.; Gao, X.; Li, B.; Liu, X.; Guan, X. Open-Phase Fault Tolerance Techniques of Five-Phase Dual-Rotor Permanent Magnet Synchronous Motor. *Energies* **2015**, *8*, 12810–12838.
15. Mariusz, M.; Marek, J.; Marian, P. Simple direct power control of Three-Phase PWM rectifier using space-vector modulation (DPC-SVM). *IEEE Trans. Ind. Appl.* **2004**, *51*, 447–454.
16. Liang, P.; Pei, Y.; Chai, F.; Zhao, K. Analytical Calculation of D- and Q-axis Inductance for Interior Permanent Magnet Motors Based on Winding Function Theory. *Energies* **2016**, *9*, 580.
17. Abdul Kadir, M.N.; Mekhilef, S.; Ping, H.W. Direct Torque Control Permanent Magnet Synchronous Motor drive with asymmetrical multilevel inverter supply. In Proceedings of the 2007 7th International Conference on Power Electronics, Daegu, Korea, 22–26 October 2007; pp. 1196–1201.

18. Sun, Z.; Li, S.; Zhang, X. Direct torque control of induction machine using finite-time control and disturbance compensation. In Proceedings of the IECON 2014—40th Annual Conference of the IEEE Industrial Electronics Society, Dallas, TX, USA, 29 October–1 November 2014; pp. 528–534.
19. Chu, J.; Hu, Y.; Huang, W. Direct active and reactive power control of PMSM. In Proceedings of the 2009 IEEE 6th International Power Electronics and Motion Control Conference, Wuhan, China, 17–20 May 2009.
20. Jacob, B.; Baiju, M.R. Spread spectrum modulation scheme for two-level inverter using vector quantised space vector-based pulse density modulation. *IET Electr. Power Appl.* **2011**, *5*, 589–596.
21. Vu, H.G.; Yahoui, H.; Chorot, T.; Hammouri, H. Control active and reactive power of Voltage Source Inverter (VSI). In Proceedings of the 2012 2nd International Symposium on Environment Friendly Energies and Applications, Newcastle upon Tyne, UK, 25–27 June 2012.
22. LaWhite, N.; Ilic, M.D. Vector space decomposition of reactive power for periodic nonsinusoidal signals. *IEEE Trans. Circuits Syst.* **1997**, *44*, 338–346.



© 2017 by the authors. Licensee MDPI, Basel, Switzerland. This article is an open access article distributed under the terms and conditions of the Creative Commons Attribution (CC BY) license (<http://creativecommons.org/licenses/by/4.0/>).